Sensors & Actuators: B. Chemical 270 (2018) 500–507

Contents lists available at ScienceDirect

Sensors and Actuators B: Chemical

journal homepage: www.elsevier.com/locate/snb

Direct laser scribing of AgNPs@RGO biochip as a reusable SERS sensor for DNA detection

Bing Han[a], Yong-Lai Zhang[a,*], Lin Zhu[a], Xu-Hui Chen[a], Zhuo-Chen Ma[a], Xu-Lin Zhang[a], Jian-Nan Wang[a], Wei Wang[a], Yu-Qing Liu[a], Qi-Dai Chen[a], Hong-Bo Sun[a,b,*]

[a] State Key Laboratory of Integrated Optoelectronics, College of Electronic Science and Engineering, Jilin University, 2699 Qianjin Street, Changchun 130012, China
[b] State Key Laboratory of Precision Measurement Technology and Instruments, Department of Precision Instrument, Tsinghua University, Haidian, Beijing 100084, China

ARTICLE INFO

Keywords:
Biochips
SERS
Laser scribing
Graphene
Silver nanoparticles

ABSTRACT

The combination of surface-enhanced Raman spectroscopy (SERS) technology with microfluidics makes it possible to diagnose genetic disease through label-free on-chip DNA detection. However, open problems including the integration of SERS substrate with microfluidic devices, controllable trapping and releasing of target molecules are still challenging. Here we demonstrate a facile laser scribing method to fabricate silver nanoparticles (AgNPs) and graphene oxide (GO) based biochips as a reusable SERS sensor for DNA detection. Programmable laser scribing of the AgNPs@GO composite film enables direct patterning of sensitive SERS channels that consist of graphene supported AgNPs by exfoliating the composites into hierarchical porous structures. Integrating the SERS-active patterns with a microfluidic chip forms a biochip for allowing SERS detection of DNA. The noncovalent interactions between DNA and graphene mediated controllable trapping and releasing of DNA sequences, enabling efficient on-chip SERS detection and the regeneration of the biochip. The simple, green and cost-effective fabrication of the SERS-active biochips reveals great potential for biomolecular sensing and genetic engineering applications.

1. Introduction

DNA analysis [1–4] that enables diagnosis of genetic disease is of great importance to molecular biology [5]. Currently, to get effective genetic structure information, various optical- [2,6,7], chemical- [8,9], electrical- [1,10], and colorimetric [11] strategies have been employed in gene detection. Generally, polymerase chain reaction (PCR) [12] and fluorescent detection [7,13] are common procedures in DNA analysis, in which the collection of specific DNA sequences enables quantitatively detecting the hybridization of the fluorophore-containing DNA, and thus the sequencing information of target DNA can be obtained. However, the intricate PCR procedure that consists of pretreatment, amplification and detection is not compatible with high-throughput on-chip DNA detection, because PCR generally requires precise and repeated temperature alteration; and thus a certain length of time is needed to complete the repeated replication of a segment of DNA. In this regard, novel DNA detection strategy that permits high-throughput on-chip analysis is highly desired.

Surface-enhanced Raman spectroscopy (SERS) features label-free fingerprint Raman spectra of analytes with ultra-high sensitivity by taking advantages of the vibrational modes of molecules [14,15]. The enhancement mechanism of SERS has been generally ascribed to the highly enhanced electromagnetic field on the metal nanostructures due to the excitation of localized surface plasmon resonance (LSPR) and the enhanced chemical interaction between target molecules and SERS substrates, in which the strong amplified electromagnetic field is dominant since it could reach an enhancement up to 10^{10} [16,17]. Recently, SERS enabled lab-on-a-chip (LoC) systems emerge as a promising approach to label-free DNA detection [4,17–19], since SERS technology permits highly sensitive detection of trace DNA sequences with fingerprint information [4,20–23]. Especially, the combination of SERS substrates with microfluidic devices [24,25] enables high-throughput on-chip analysis with low sample consumption, high sensitivity and specificity to target molecules, revealing great potential for gene diagnosis. As typical examples, Zhao et al. fabricated an on-chip SERS system with silver nanoparticles (AgNPs)/Si nanopillar array embedded in microfluidic channels [26,27], exhibiting an excellent performance in detecting double strand DNA. Luke P. Lee et al. reported a high-density Ag nanoparticle film, which successfully tuned the particle spacing with controllable SERS detection [23]. Besides, on-chip

* Corresponding authors at: State Key Laboratory of Integrated Optoelectronics, College of Electronic Science and Engineering, Jilin University, 2699 Qianjin Street, Changchun 130012, China.
E-mail addresses: yonglaizhang@jlu.edu.cn (Y.-L. Zhang), hbsun@tsinghua.edu.cn (H.-B. Sun).

https://doi.org/10.1016/j.snb.2018.05.043
Received 30 January 2018; Received in revised form 8 May 2018; Accepted 9 May 2018
Available online 25 May 2018
0925-4005/

SERS detection has been achieved based on various SERS enabled LoC platforms, such as microfluidic channels equipped with roughed-Au layers [28,29], aluminum nanocrystals [30], silver nanoplates [31], and nanogaps-rich gold nanomaterial [32,33].

Despite the aforementioned advances in recent years, on-chip SERS detection of DNA still suffers from series of problems. First, it is technically challenging to integrate efficient SERS substrates within a microfluidic chip, since the traditional strategies for producing SERS substrates are 2D technologies that are not compatible with non-planar microfluidic channels; second, owning to the low Reynolds number, flowing fluids in micro-channels become laminar. A key consequence is target biomolecules do not necessarily interact with the SERS substrates through diffusion, thus high-efficiency trapping strategy is essential for sensitive DNA detection [34]; third, most of the SERS chips suffer from poor reusability [35], residual biomolecules on the SERS substrate would cause cross contamination, interfering the next experiments. In this regard, the development of reusable SERS-active bio-chips that enable controllable trapping and releasing of biomolecules is still a challenging task.

We report here a facial laser scribing [36,37] of AgNPs and graphene oxide (GO) composites (AgNPs@GO) for the fabrication of SERS-active biochips towards DNA detection. AgNPs@GO composites were prepared by UV irradiation induced photoreduction of $Ag(NH_3)^+$ and GO in aqueous solution [38]. Programmable laser scribing of the AgNPs@GO composite film enables direct writing arbitrarily shaped patterns that consist of AgNPs and reduced GO (AgNPs@RGO), since the laser treated region has been exfoliated into hierarchical porous structures. By transferring the channel-shaped AgNPs@RGO patterns to a pre-designed PDMS-based microfluidic chip through general stamping method, a SERS-active biochip has been successfully developed. The laser exfoliated RGO foam not only serves as nanoporous scaffold for AgNPs [38,39], but also acts as an active substrate that shows strong interaction with target biomolecules such as DNA sequences [6,13,34]. The closely packed AgNPs on graphene sheets can electromagnetically enhance the Raman signal [40–42] due to coupling of localized surface plasmon resonances of adjacent nanoparticles [17,31,43]. Thus the AgNPs@RGO biochip can work as a SERS sensor for on-chip DNA detection. The noncovalent interaction [13,34] between DNA and graphene can be employed to selective trapping and releasing of target DNA sequences, which not only promotes the sensitivity of this SERS sensor, but also makes it reusable [44,45]. Direct laser scribing of AgNPs@RGO-based SERS sensor reveals great potential for developing sensitive, portable and reusable biochips.

2. Experiments

2.1. Preparation of AgNPs@GO composite material

AgNPs@GO composite materials were fabricated by one step photoreduction method. $NH_3{\cdot}H_2O$ (Sigma-Aldrich Co.) was slowly dropped into 10 mL of $AgNO_3$ solution (Sigma-Aldrich Co., 1 mM) under magnetic stirring (800 rpm) until the precipitates disappeared. The suitable amount of ammonia was added to form clear $Ag(NH_3)_2^+$ first. The obtained $Ag(NH_3)_2OH$ was mixed with 10 mL of GO solution (4 mg/mL), which was prepared by a modified Hummer's method. The resulting solution was irradiated under UV-light (500 W, Philips, QVF135) for 10 min, under stirring. The AgNPs@GO solution was formed and washed with deionized water for 3 times. Then the composite materials were re-dissolved in 20 mL of deionized water.

2.2. Laser scribing of AgNPs@GO film

The laser-scribe approach, which belongs to continuous laser direct writing method, is based on a 780 nm focused near-infrared laser (200 mW) within a DVD drive. The DVD can be located and written repeatedly by Nero StartSmart Essentials, and it could be used to realize a large-area, fast and maskless reduction of GO. Only 20 min were required for the entire patterning of the front cover of a DVD disc. In our experiment, the AgNPs@GO composite solution was directly cast onto DVD disc. After drying under ambient condition, the stack and flat films were formed on the disc with an average thickness of 2 μm. Then the disc was inserted into the laser-scribe DVD drive. The pre-programmed channel patterns could be directly "written" onto the composite film, forming foam-like AgNPs@RGO structures.

2.3. Fabrication of the SERS-active biochip

Our biochip is composed of a PDMS (Sylgard 184 Silicone Elastomer, Dow Corning Corporation) microfluidic channel and a flat PDMS substrate integrated with the same AgNPs@RGO channel patterns. The AgNPs@RGO based channel pattern prepared by laser scribing was selectively transferred to the PDMS channel, and the magnified SEM image showed that the transferred substrate retained the loose and exfoliated morphology (Fig. S1). Meanwhile, the region without laser-scribe treatment could not be lifted-off due to the compact stack of graphene layers. The bare PDMS surface facilitated the follow-up sealing with channels. After exposure to air plasma, tight covalent bonds were formed between two conformal layers, ultimately making an enclosed SERS-active biochip. Through this simple procedure, a flexible AgNPs@RGO biochip was obtained.

2.4. Electric field simulation of the AgNPs array on graphene sheet

The electric field distribution of the AgNPs on graphene sheet was simulated by the finite difference time domain method (FDTD). The AgNPs@RGO composite material was simplified into two-dimensional case. The AgNPs were adjusted with an average diameter of nearly 5 nm, and the nanogaps between particles were set to be ~2 nm. Localized surface plasmon resonance was excited by 532 nm wavelength light excitation around AgNPs. The LSPR was coupled with one another between two adjacent particles; thereby the electromagnetic field could be enhanced by 200.

2.5. Characterizations

The SEM images of the samples were measured using a JEOL JSM-7500F field emission scanning electron microscope. X-ray photoelectron spectroscopy (XPS) was performed using an ESCALAB 250 spectrometer (Thermo Fisher Scientific, USA). XRD data were recorded on a Rigaku D/Max-2550 diffractometer with Cu Kα radiation (λ = 0.15418 nm). Surface enhanced Raman spectra were measured on a JOBIN YVON T64000 equipped with a liquid-nitrogen-cooled argon ion laser at 532 nm (Spectra-Physics Stabilite 2017) as an excitation source. The laser power was ~30 μW on the samples, and the average spot size was 1 μm in diameter using a long-working distance 50× objective. The ssDNAs were purchased from Takara Bio Incorporated (Otsu, Shuga, Japan). The samples were dissolved in phosphate buffer (1 nM). SERS spectra were collected with 5 s exposure time, 3 accumulations. CLSM images were obtained using an LEXT 3D measuring laser microscope (OLS4100).

3. Results and discussion

To develop a facile strategy to fabricate a SERS-active DNA biochip, a laser scribing technology [36] was employed to make AgNPs@RGO SERS substrate. Fig. 1a shows the fabrication procedure of the AgNPs@RGO biochip. First, AgNPs@GO composite material was prepared through one-step UV-photoreduction of an aqueous mixture of silver-ammonia and GO [38]. Herein, to prevent uncontrollable chemical reduction of both GO and silver ions, a suitable amount of ammonia was added to form clear $Ag(NH_3)_2OH$ solution. The formation mechanism of AgNPs on GO sheet under UV irradiation is illustrated in

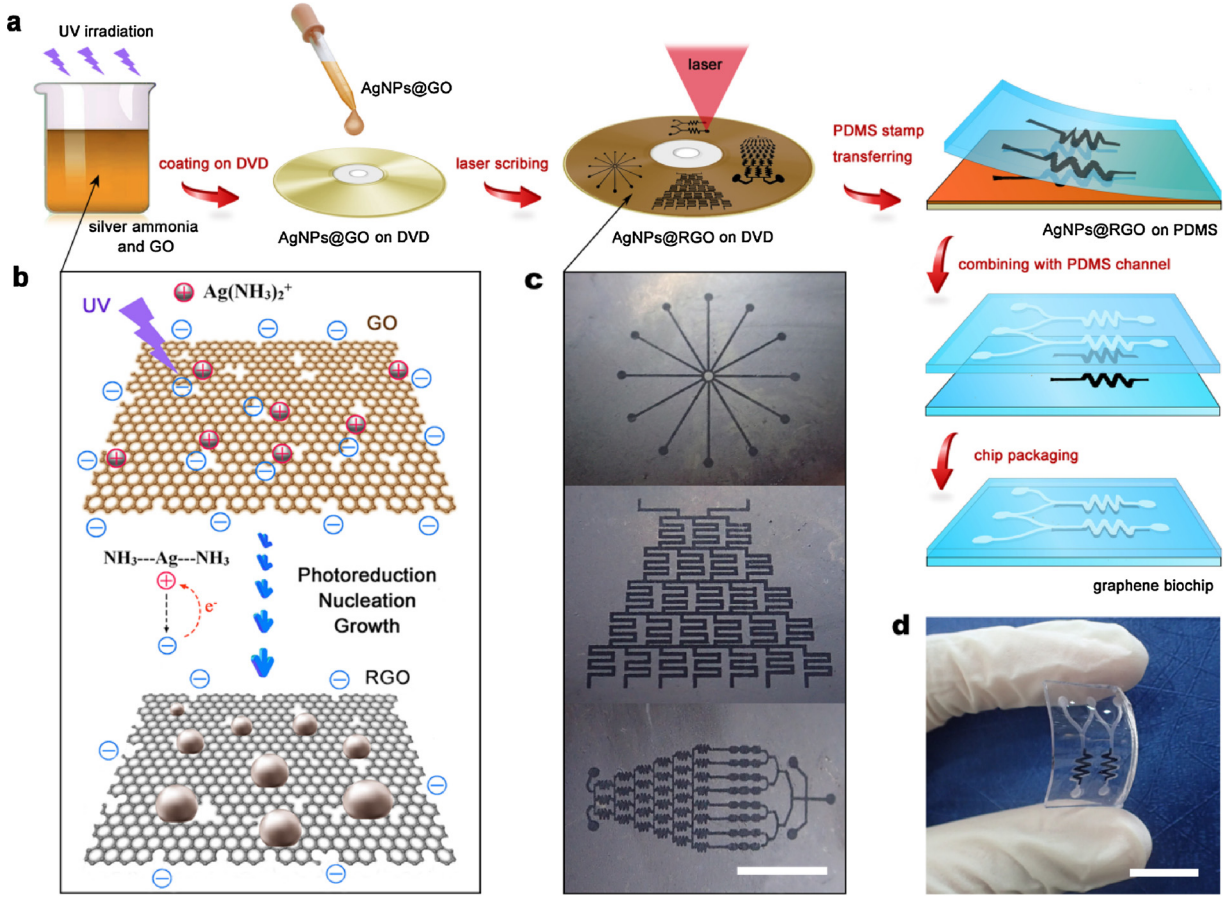

Fig 1. Fabrication of AgNPs@RGO biochip. (a) Schematic illustration of the fabrication procedure of an AgNPs@RGO SERS biochip. (b) The mechanism of AgNPs growth onto graphene sheets upon UV irradiation. (c) Programmable patterning of various AgNPs@RGO SERS substrates for biochip assembly. Scale bar: 500 μm. (d) Photograph of the as-prepared AgNPs@RGO SERS biochip. Scale bar: 1 cm.

Fig. 1b. Briefly, the cationic $Ag(NH_3)_2^+$ absorbed onto the negatively charged GO surface due to the electric interaction [39] can be reduced into silver under UV irradiation. Since the capped NH_3 groups prevented the Ag nucleus from aggregating, the as-formed AgNPs can anchor onto the graphene sheets with high dispersibility and uniformity [38]. Second, the as-prepared AgNPs@GO solution was casted on to a DVD disc that permits Light-Scribing [37]. After drying naturally, a computer-designed pattern of the biochip channel network was directly written on the AgNPs@GO composite film. After laser treatment, black channel patterns could be observed due to the photoreduction of GO. Herein, we have to point out that the UV–vis absorption spectrum of the GO showed that it has poor light absorption in the near-infrared region. Additionally, the power of laser in the DVD driver is pretty low (780 nm, 200 mW). Hence, to trigger complete reduction of GO film, it generally needs to scan the sample for several times. In our work, the surface plasmon of AgNPs could significantly promote the reduction degree. When 780 nm laser irradiated the AgNPs, the surface plasmon can be excited (Fig. S2). The oscillation of the surface plasmon can help to convert light into heat, which facilitates the deoxidation process. In the case of GO, the oxygen containing groups (OCGs) can be removed slightly after laser scribing for only one time. In contrast, the OCGs of the AgNPs@GO composite were removed dramatically after laser scribing at the same condition (Fig. S3). The reduction degree of GO and AgNPs@RGO films can be easily distinguished by naked eyes (Fig. S4). These results confirm the advantage of our modified laser scribing technology.

By taking advantage of the "direct writing" feature [46], any desired microfluidic channels patterns can be created on the AgNPs@GO films (Fig. 1c). Unlike conventional photolithography, the light-scribe technique enable one-step patterning of graphene without the use of masks and expensive instruments. In this regard, it is a cost-effective and scalable method for chip fabrication. Using a simple stamping method, the AgNPs@RGO channel patterns can be selectively transferred to polydimethylsiloxane (PDMS) slice for chip fabrication. Then, another PDMS slice with the same channel pattern was covered over the AgNPs@RGO patterns, forming a sealed PDMS chip with embedded AgNPs@RGO SERS substrate (Fig. 1d).

It is well known that GO could be reduced into RGO using various light sources [47], including UV irradiation [48], flash lamp [49], sunlight [50], and lasers [36,37]. We adopted laser scribing strategy using a near-infrared (NIR) laser (788 nm) of a standard LightScribe DVD optical drive, because the laser scribing reduction of GO can induce a highly porous structure. As shown in the scanning electron microscope (SEM) image (Fig. 2a), the laser-scribing treatment break the continuous GO film into small pieces and exfoliated the stacked GO film into a porous structure; whereas the untreated region remained smooth and flat. This apparent morphology change was of benefit to subsequent transfer of the AgNPs@RGO composite to PDMS substrate. Laser scanning confocal microscopy (LSCM) image confirms the exfoliated structure of the AgNPs@RGO region; an expanded surface formed along the laser scanning path due to the rapid degassing of oxygen containing groups (OCGs, eg., carbonyl, epoxy and hydroxyl groups) (Fig. S5). The laser scribing technology enable precise patterning, the resolution of a single line can reach 20 μm, which is precise enough for most of microfluidic channels (Fig. 2b). The AgNPs from on graphene layers were closely and uniformly packed with narrow gaps of ~2 nm (Fig. 2c), which can produce intense "hot spots" [17,26,27] for SERS detection. More importantly, the hierarchically porous structure can make more

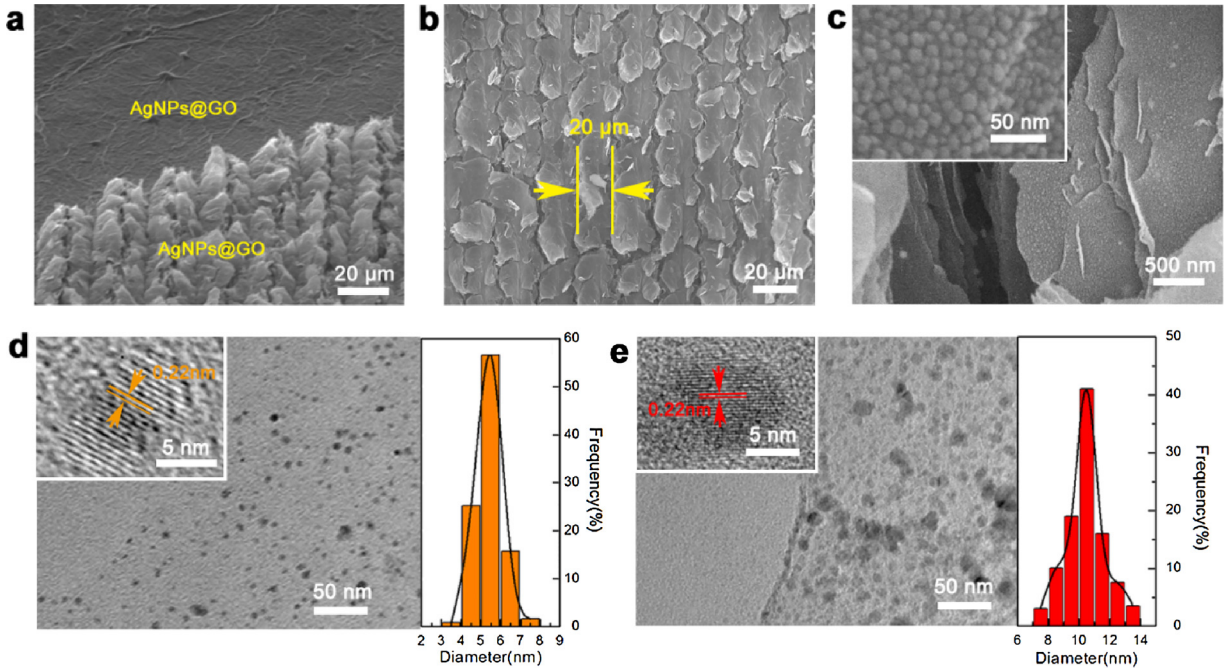

Fig. 2. Surface morphologies of AgNPs@RGO. (a) SEM image of laser scribed AgNPs@RGO film. (b) Top-view SEM image of AgNPs@RGO. (c) High-resolution SEM images of exfoliated AgNPs@RGO foam, the inset is the SEM of AgNPs closely packed on the surface of graphene sheets. (d) TEM image of AgNPs@GO and the size distribution of AgNPs decorated on graphene sheet. The inset is the HRTEM image of an AgNP. (e) TEM image of AgNPs@RGO and the size distribution of AgNPs on graphene sheets after laser treatment, the inset is the HR-TEM image of an AgNP.

SERS "hot spots" exposed to the environment and thus facilitate the adsorption/desorption of biomolecules, promoting the sensitivity.

Transmission electron microscopy (TEM) images gave a clear comparison of the AgNPs before and after laser treatment. Notably, the as-formed AgNPs decorated on GO sheet shows an average diameter of ~5.5 nm (Fig. 2d). The density of AgNPs on graphene sheet could be tuned by changing the UV irradiation time [38] (Fig. S6). After laser treatment, the AgNPs grew bigger due to NIR-laser induced thermal coalescence effect (Fig. 2e). The average diameter increased to ~11 nm. High-resolution TEM (HRTEM) image (inset of Fig. 2e) indicates the crystalline lattices of (111) phases (d = 0.23 nm) of Ag^0, which kept unchanged during laser scribing.

In addition to the effects on AgNPs, further analysis has been carried out to make a comprehensive comparison of the property/structural changes of GO before and after laser scribing. The X-ray photoelectron spectroscopy (XPS) of C1 s peaks was collected to investigate the carbon/oxygen (C/O) atom ratio variation. The C1 s spectra could be resolved into three peaks, representing C—C (284.6 eV), C—O (~286.6 eV, epoxy and hydroxyl groups) and C═O (~288.5 eV, carbonyl groups), respectively (Fig. 3a). After UV reduction, the C—O and C═O contents of the AgNPs@GO composite decreased obviously as compared with that of pristine GO, indicating that the OCGs were partially removed. The C/O mass ratio slightly increased from 1.4 (GO) to ~3.5 (AgNPs@GO). After laser scribing treatment, the OCGs of the AgNPs@RGO sample was further removed, leading to a high C/O mass ratio of ~42. The survey spectra of GO, AgNPs@GO and AgNPs@RGO given a comprehensive comparison of O 1s and C 1s peaks changes (Fig. S7). It was reported that RGO sheets have much stronger interaction with DNA sequences than that with pristine graphene [51–53]. According to the literature results, the molecules adsorbed on the GO and RGO sheet is almost the same [51], since both π-π interaction and hydrogen bonding may contribute to the interaction between guest molecules and GO/RGO. In the case of ssDNA molecules, they can interact with graphene domain mainly through noncovalent binding. For GO, the presence of OCGs can interrupt the large sp^2 domains, which may more or less depress their interaction. However, the laser reduction of GO can partially recover the sp^2 domains, and thus offering much stronger interaction rate than GO. In this regard, reduction of GO is more beneficial for trapping of biomolecules such as DNA, further promoting the sensitivity of the resultant biochips.

The Raman spectra of GO, AgNPs@GO, AgNPs@RGO is shown in Fig. 3b. Typical *D* and *G* bands round at 1350 cm^{-1} and 1580 cm^{-1} that reflect disorders/edges in the sp^2 domain and the E_{2g} phonon of C sp^2 atoms can be observed all over these three samples. After UV irradiation, the intensity of *D*-band of AgNPs@GO sample decreased obviously due to the reconstruction of sp^2 domain. After laser scribing treatment, the D-band intensity increased slightly, which can be attributed to the cutting and exfoliation of the graphene sheets, which induced more dangling bonds at the edge of small sheets. However, the overall peak narrowing of D and G bands indicated the decrease in defect types, suggesting the removal of OCGs. In addition, the AgNPs@GO and AgNPs@RGO composites presented an obvious increase in Raman signal intensity, nearly one order of magnitude. This phenomenon was consistent with the SERS charge transfer effect between AgNPs and RGO.

XRD patterns show that the layered structure of GO becomes disordered after the formation of AgNPs and the laser scribing treatment (Fig. 3c), since typical diffraction peak at 11° disappeared in the XRD patterns of AgNPs@GO and AgNPs@RGO samples. The removal of OCGs helps to restore the graphitic crystal phase that related to the (200) plane of RGO. In addition, the diffraction peaks that corresponds to the (111), (200) and (220) plane of the silver face center cubic structure appear at 38.7°, 44.7° and 65.1°, respectively [38], which suggests the presence of AgNPs in the samples of AgNPs@GO and AgNPs@RGO.

Finite-difference time-domain (FDTD) simulation has been adopted to investigate the electromagnetic field enhancement of the AgNPs@RGO substrate (Fig. 4a). The simulation of the AgNPs structures was based on the real morphology of AgNPs@RGO shown in the inset of Fig. 2c. The AgNPs are close-packed on graphene sheet in a dense arrangement with diameter nearly 10 nm. The coupling of localized surface plasmon resonances [43,54] of adjacent nanoparticles was found

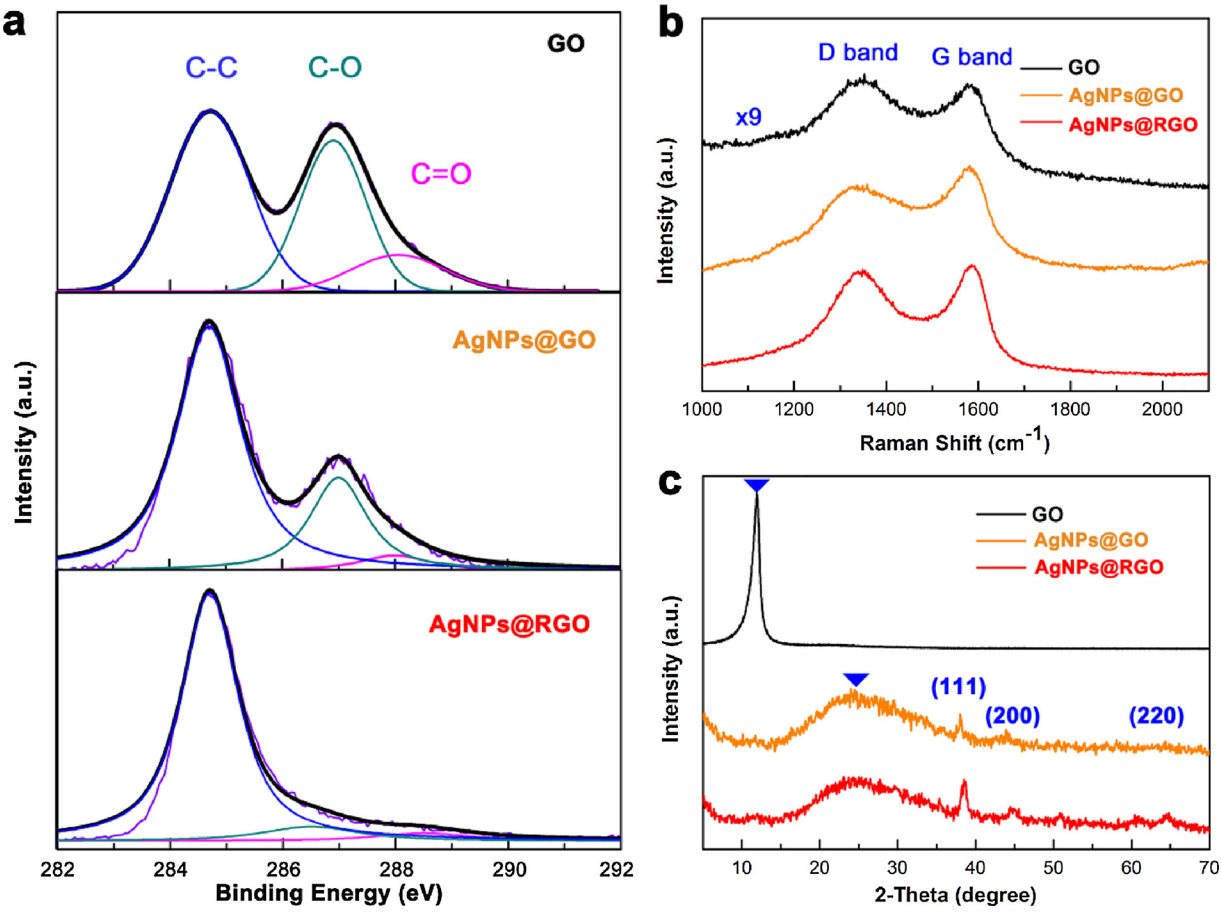

Fig. 3. (a) C1s XPS spectra, (b) Raman spectra and (c) XRD patterns of GO, AgNPs@GO and AgNPs@RGO samples.

to be essential for achieving high SERS enhancement [41,55]. For two adjacent AgNPs, the electrons can be enriched at a relatively large space between the electron clouds of their outer orbits; whereas, for AgNPs decorated on graphene, due to the lower overall energy of its electron orbit, a great number of electrons are confined within a much smaller region, probably at their interface, thus creating a significantly enhanced electromagnetic field. According to our results, the maximum electric field enhancement (E/E_0) can reach 200 times, which can lead to significant enhancement in SERS signal, since the enhancement factor is theoretically proportional to $|E/E_0|^4$ [17]. As a control experiment, we compared the SERS performance of AgNPs@RGO substrate with AgNPs@GO (before laser scribing) and laser scribed RGO films without loading AgNPs (Fig. 4b). By using 10^{-6} M of R6G as the probe molecule, the AgNPs@RGO substrate shows the highest SERS enhancement, confirming the unique advantage of combining AgNPs with graphene. More importantly, the intensity of SERS signal was proportional to the amount of molecules adsorbed on the SERS substrate, the intensity of the SERS spectra decrease when the concentrations of R6G decrease. The LOD can reach 10^{-10} M (Fig. 4c). The SERS peaks at 1353 and 1509 cm^{-1} are related to the aromatic and aliphatic C—C stretching modes in R6G, respectively. According to the calculation formula

$$EF = \frac{I_{SERS} \times N_{bulk}}{N_{SERS} \times I_{bulk}}$$

where I_{SERS} is the vibrational intensity of a mode in the surface enhanced Raman spectrum, I_{bulk} is the intensity of the same mode in the Raman spectrum, N_{SERS} is the number of molecules adsorbed on the substrate within the laser spot area, and N_{bulk} is the number of molecules excited within the volume of the laser waist in a bulk sample

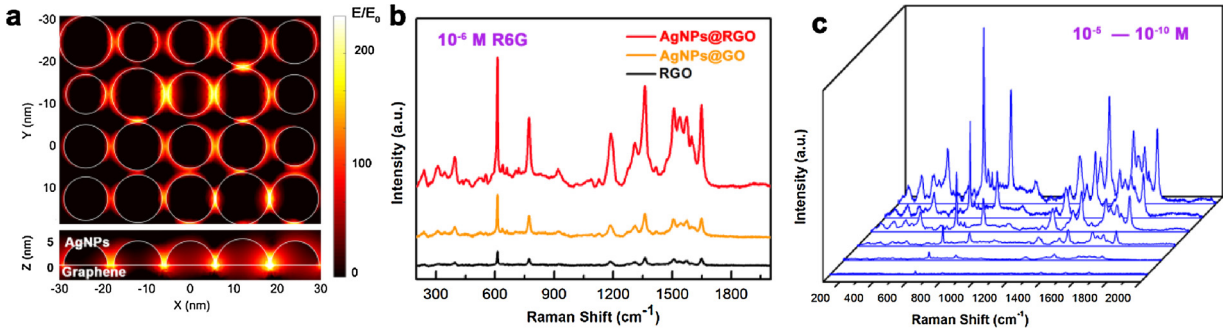

Fig. 4. (a) FDTD stimulation of the electric field distribution of compact Ag array assembled on graphene layer. (b) SERS spectra of R6G molecules detected on different substrates. (c) SERS spectra of R6G with different concentration from 10^{-5} to 10^{-10} M.

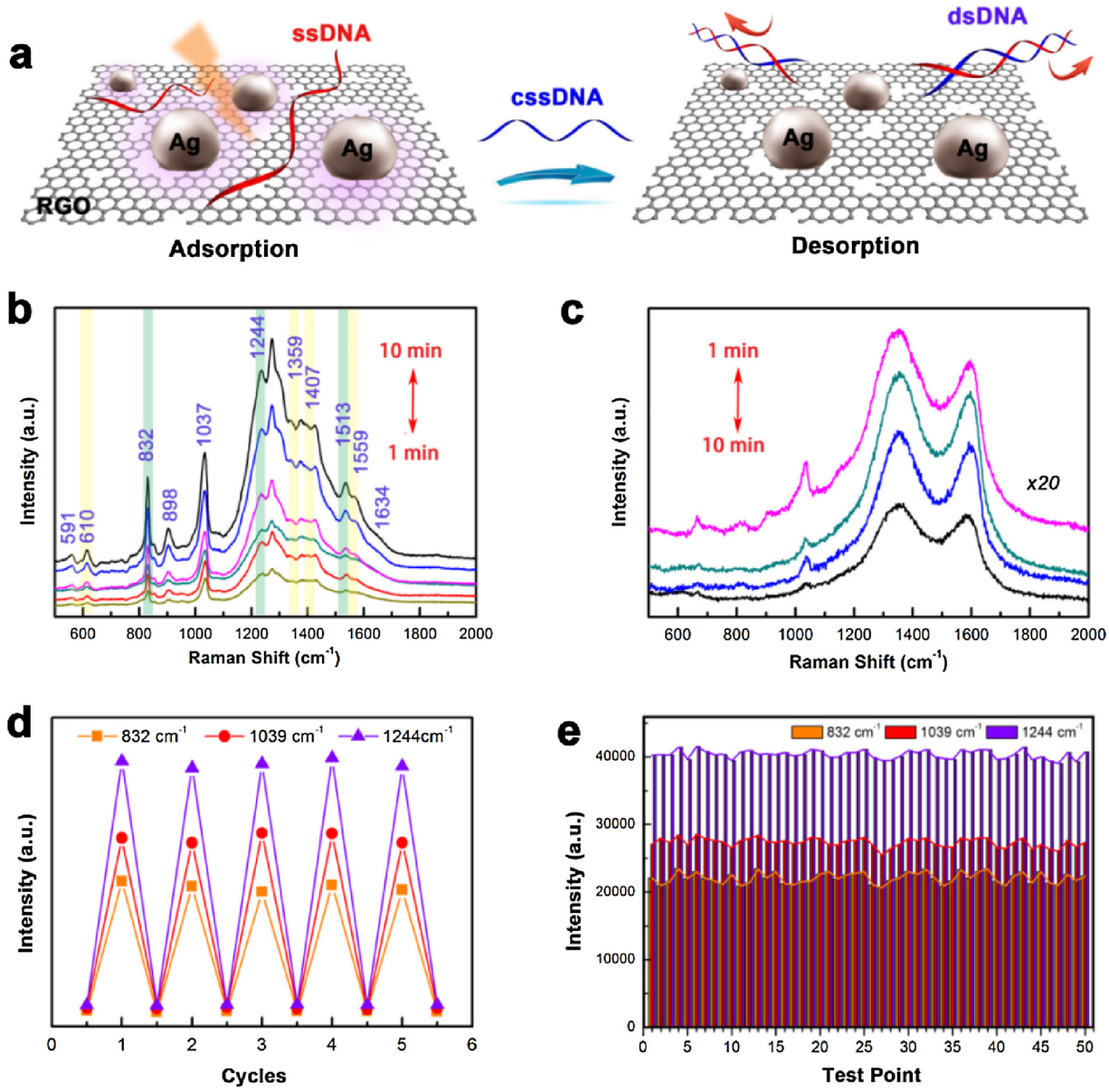

Fig. 5. (a) Schematic illustration of the DNA trapping and releasing mechanism on AgNPs@RGO substrate. (b) SERS spectra of a 30-base ssDNA sequence with increasing injection time (from 1 min to 10 min, with a concentration of 10^{-6} M unchanged). (c) SERS spectra in the presence of the cssDNA sequence injected into the channel. (d) Reusability of the biochip for five cycles of DNA SERS detection. (e) Reproducibility of biochips for detection measured at 50 different points.

[16,31]. In our result of AgNPs@RGO substrate, the EF value was estimated to be nearly 8.9×10^8.

The graphene and AgNPs composites can act an excellent platform for SERS detection of biomolecules such as DNA, since the noncovalent binding affinity between single-stranded DNA (ssDNA) and graphene sheets together with the strong interaction between complementary ssDNA (cssDNA) can be well employed for controllable trapping and detachment of target DNA sequences (Fig. 5a). Such a ssDNA and graphene interaction has been previously used in the fluorescent detection of DNA [13], in which theoretical and experimental results show that ssDNA sequences are directly lying on graphene layer with all nucleobases flat to favor π-π stacking between the bases and aromatic carbons in graphene. However, in the presence of a cssDNA, the formation of double-stranded DNA (dsDNA) will hide the base within the double helix, which disturb the interaction between ssDNA and graphene, thus a controllable detachment of the target can be realized. The controllable adsorption and desorption of DNA sequences is of benefit to the trapping and detachment of targets, thus making the SERS substrates not only sensitive but also reusable [44].

In this work, we integrated the AgNPs@RGO with a PDMS microfluidic chip which was designed as an efficient SERS sensor for on-chip DNA detection. When the injected ssDNA solution passed over the AgNPs@RGO substrate in the channel, DNA sequences can be attached to the graphene sheet. The expanded foam structure of graphene was favorable to expose much larger surface to the microfluids, and thus the capillary force and strong noncovalent binding between DNA sequences and graphene benefited the trapping of more target molecules. Here, it is worthy pointing out that the trapping of biomolecules is of great importance to the on-chip SERS detection, because the flowing fluids may become laminar at the microscale, and thus the target biomolecules do not necessarily interact with the embedded SERS substrates without efficient trapping, resulting in poor sensitivity.

To validate our proposed method, we carried out the on-chip SERS detection experiments. We kept the concentration of a 30-base ssDNA samples at 10^{-6} M, and measure the SERS signal changes with time. Obvious SERS signals can be detected within 1 min (Figs. 5b and S8).

The SERS signals enhanced with the increase of time due to the trapping of more ssDNA molecules. Typical bands at 832, 1244 and 1513 cm^{-1} were assigned to poly C, while the bands at 610, 359, 1407 and 1559 cm^{-1} were related to poly G. Although, the D band and G band of RGO can be also detected, the two broad peaks do not overlap the signature of DNA molecules. Given that the ssDNA sequences contained poly A, C, T, G with the ratio of 7:9:7:7, the SERS signals cover all of these bases information. In addition, the sensitive on-chip SERS detection enables detecting DNA sequences with small variations of molecular structures, revealing the potential for real gene detection. As a proof of concept, we also tested the cssDNA sequences (the A, C, T, G ratio: 7:7:7:9). SERS spectra tested at different time were shown in Fig. S9. Most of the band appeared unchanged, but the bands related to poly C were lower, and the bands assigned to poly G were enhanced as compared with the ssDNA sequences, in good consistent with the proportion of the four bases. The SERS signals of ssDNA adsorbed on AgNPs@RGO, AgNPs and RGO substrates are investigated (Fig. S10). Experimental conditions have been carefully controlled to make their particle sizes, reduction time, film thicknesses and concentration of ssDNA comparable. The RGO sensor produces a relatively weak signal, since the chemical enhancement of SERS signal is much lower as compared with electromagnetic enhancement derived from AgNPs. SERS signal detected based on AgNPs is relative weak due to the weak interaction between the substrate and ssDNA. The signal obtained by AgNPs@RGO sensor is superior to the other two substrates due to the synergistic effect of the electromagnetic enhancement and strong interaction between DNA and graphene.

Besides, the reusability of the AgNPs@RGO biochip is also an attractive feature. By making full use of the competitive noncovalent interaction between graphene-ssDNA and ssDNA-cssDNA, the trapped ssDNA sequences can be washed away from the AgNPs@RGO substrate, in this way, the SERS sensor can be regenerated for cycling usage. After injecting the cssDNA into the channels, the SERS signal of the previously trapped ssDNA decreased with the increase of interaction time. The SERS signal of ssDNA disappeared after 10 min, indicating the regeneration of the SERS chip (Fig. 5c). To evaluate the reusability of our AgNPs@RGO biochip, another five rounds of ssDNA detection have been carried out. Notably, during five cycles of detection and regeneration, the intensity of three typical bands at 832, 1039, and 1244 cm^{-1} can be switched reversibly. Moreover, the SERS enhancement almost keeps a constant value, indicating the very stable performance during recycled usage (Fig. 5d).

The uniform distribution of AgNPs on the graphene sheets can also guarantee reasonable signal reproducibility. Experiments were performed to confirm the reproducibility by randomly detecting the ssDNA molecules at 50 different points. As shown in Fig. 5e, these 50 spectra demonstrated superior homogeneity, indicating the good reproducibility. Very low relative standard deviation (RSD) of 4.3%, 4.2% and 5.1% has been achieved with respect to the characteristic peaks at 832 cm^{-1}, 1244 cm^{-1}, 1537 cm^{-1}, respectively. The superior signal reproducibility render the biochip reliable performance in real clinical applications.

4. Conclusions

In summary, a high-efficiency and reusable SERS-active biochip has been fabricated through a facile and low-cost laser scribing treatment of AgNPs@GO composites. Arbitrarily shaped patterns can be directly "written" on the composite film due to the laser induced exfoliation and reduction of GO, which facilitates the design and fabrication of SERS-active biochips consisting of graphene supported AgNPs. Since the biomolecules interact noncovalently with graphene material, controllable trapping and releasing of DNA sequences can be achieved, which not only promotes the sensitivity of the SERS detection of DNA, but also makes it possible to regenerate the biochips for reusage. As a typical demonstration, on-chip SERS detection of a 30-base ssDNA samples at 10^{-6} M can be realized within 1 min. Additionally, reasonable high SERS signal reproducibility and low RSD of ~5% has been achieved. The AgNPs@RGO based biochips hold great promise for high-throughput on-chip detection of biomolecules.

Acknowledgment

The authors would like to acknowledge the National Key Research and Development Program of China and National Natural Science Foundation of China (NSFC) under Grant #2017YFB1104300 , #61522503, #61775078, #61590930, and 2014CB921302 for support.

Appendix A. Supplementary data

Supplementary data associated with this article can be found, in the online version, at https://doi.org/10.1016/j.snb.2018.05.043.

References

[1] S. Xu, J. Zhan, B. Man, S. Jiang, W. Yue, S. Gao, C. Guo, H. Liu, Z. Li, J. Wang, Y. Zhou, Real-time reliable determination of binding kinetics of DNA hybridization using a multi-channel graphene biosensor, Nat. Commun. 8 (2017) 14902–14911.
[2] V.V. Thacker, L.O. Herrmann, D.O. Sigle, T. Zhang, T. Liedl, J.J. Baumberg, U.F. Keyser, DNA origami based assembly of gold nanoparticle dimers for surface-enhanced Raman scattering, Nat. Commun. 5 (2014) 3448–3452.
[3] A. Barhoumi, D. Zhang, F. Tam, N.J. Halas, Surface-enhanced raman spectroscopy of DNA, J. Am. Chem. Soc. 130 (2008) 5523–5529.
[4] G.L. Liu, Y. Yin, S. Kunchakarra, B. Mukherjee, D. Gerion, S.D. Jett, D.G. Bear, J.W. Gray, A.P. Alivisatos, L.P. Lee, F.F. Chen, A nanoplasmonic molecular ruler for measuring nuclease activity and DNA footprinting, Nat. Nanotechnol. 1 (2006) 47–52.
[5] K. Ariga, H. Ito, J.P. Hill, H. Tsukube, Molecular recognition: from solution science to nano/materials technology, Chem. Soc. Rev. 41 (2012) 5800–5835.
[6] L. Feng, L. Wu, X. Qu, New horizons for diagnostics and therapeutic applications of graphene and graphene oxide, Adv. Mater. 25 (2013) 168–186.
[7] F.B. Myers, L.P. Lee, Innovations in optical microfluidic technologies for point-of-care diagnostics, Lab Chip 8 (2008) 2015–2031.
[8] T.G. Drummond, M.G. Hill, J.K. Barton, Electrochemical DNA sensors, Nat. Biotechnol. 21 (2003) 1192–1199.
[9] A. Karabchevsky, A. Mosayyebi, A.V. Kavokin, Tuning the chemiluminescence of a luminol flow using plasmonic nanoparticles, Light Sci. Appl. 5 (2016) e16164–e16164.
[10] S.J. Park, T.A. Taton, C.A. Mirkin, Array-based electrical detection of DNA with nanoparticle probes, Science 295 (2002) 1503–1506.
[11] H.N. Kim, W.X. Ren, J.S. Kim, J. Yoon, Fluorescent and colorimetric sensors for detection of lead, cadmium, and mercury ions, Chem. Soc. Rev. 41 (2012) 3210–3244.
[12] T.D. Schmittgen, K.J. Livak, Analyzing real-time PCR data by the comparative C-T method, Nat. Protoc. 3 (2008) 1101–1108.
[13] C.H. Lu, H.H. Yang, C.L. Zhu, X. Chen, G.N. Chen, A graphene platform for sensing biomolecules, Angew. Chem., Int. Ed. Engl. 48 (2009) 4785–4787.
[14] S. Chen, B. Liu, X. Zhang, Y. Mo, F. Chen, H. Shi, W. Zhang, C. Hu, J. Chen, Electrochemical fabrication of pyramid-shape silver microstructure as effective and reusable SERS substrate, Electrochim. Acta 274 (2018) 242–249.
[15] M. Fan, G.F. Andrade, A.G. Brolo, A review on the fabrication of substrates for surface enhanced Raman spectroscopy and their applications in analytical chemistry, Anal. Chim. Acta 693 (2011) 7–25.
[16] Z.-C. Ma, Y.-L. Zhang, B. Han, X.-Q. Liu, H.-Z. Zhang, Q.-D. Chen, H.-B. Sun, Femtosecond laser direct writing of plasmonic Ag/Pd alloy nanostructures enables flexible integration of robust SERS substrates, Adv. Mater. Technol. 2 (2017) 1600270.
[17] J.-A. Huang, Y.-L. Zhang, H. Ding, H.-B. Sun, SERS-enabled lab-on-a-chip systems, Adv. Opt. Mater. 3 (2015) 618–633.
[18] I.J. Jahn, O. Zukovskaja, X.S. Zheng, K. Weber, T.W. Bocklitz, D. Cialla-May, J. Popp, Surface-enhanced Raman spectroscopy and microfluidic platforms: challenges, solutions and potential applications, Analyst 142 (2017) 1022–1047.
[19] H. Wang, Y.-L. Zhang, W. Wang, H. Ding, H.-B. Sun, On-chip laser processing for the development of multifunctional microfluidic chips, Laser Photon. Rev. 11 (2017) 1600116.
[20] J.F. Li, Y.F. Huang, Y. Ding, Z.L. Yang, S.B. Li, X.S. Zhou, F.R. Fan, W. Zhang, Z.Y. Zhou, D.Y. Wu, B. Ren, Z.L. Wang, Z.Q. Tian, Shell-isolated nanoparticle-enhanced raman spectroscopy, Nature 464 (2010) 392–395.
[21] D.K. Lim, K.S. Jeon, H.M. Kim, J.M. Nam, Y.D. Suh, Nanogap-engineerable Raman-active nanodumbbells for single-molecule detection, Nat. Mater. 9 (2010) 60–67.
[22] E. Prado, A. Colin, L. Servant, S. Lecomte, SERS spectra of oligonucleotides as fingerprints to detect label-free RNA in microfluidic devices, J. Phys. Chem. C 118 (2014) 13965–13971.
[23] Y. Lu, G.L. Liu, L.P. Lee, High-density silver nanoparticle film with temperature-controllable interparticle spacing for a tunable surface enhanced Raman scattering substrate, Nano Lett. 5 (2005) 5–9.

[24] B.B. Xu, R. Zhang, X.Q. Liu, H. Wang, Y.L. Zhang, H.B. Jiang, L. Wang, Z.C. Ma, J.F. Ku, F.S. Xiao, H.B. Sun, On-chip fabrication of silver microflower arrays as a catalytic microreactor for allowing in situ SERS monitoring, Chem. Commun. 48 (2012) 1680–1682.
[25] W. Yan, L. Yang, J. Chen, Y. Wu, P. Wang, Z. Li, In situ two-step photoreduced SERS materials for on-chip single-molecule spectroscopy with high reproducibility, Adv. Mater. 29 (2017).
[26] Y. Zhao, J.-A. Huang, Z. Zhang, X. Chen, W. Zhang, Quantitative analysis of multiplex-components and double stranded DNA by wide-range surface-enhanced Raman spectroscopy based on ordered Ag/Si nanowire arrays, J. Mater. Chem. A 2 (2014) 10218–10224.
[27] J.A. Huang, Y.Q. Zhao, X.J. Zhang, L.F. He, T.L. Wong, Y.S. Chui, W.J. Zhang, S.T. Lee, Ordered Ag/Si nanowires array: wide-range surface-enhanced Raman spectroscopy for reproducible biomolecule detection, Nano Lett. 13 (2013) 5039–5045.
[28] W. Hüttner, K. Christou, A. Göhmann, V. Beushausen, H. Wackerbarth, Implementation of substrates for surface-enhanced Raman spectroscopy for continuous analysis in an optofluidic device, Microfluidics Nanofluidics 12 (2011) 521–527.
[29] Q. Sun, K. Ueno, H. Yu, A. Kubo, Y. Matsuo, H. Misawa, Direct imaging of the near field and dynamics of surface plasmon resonance on gold nanostructures using photoemission electron microscopy, Light Sci. Appl. 2 (2013) e118–e118.
[30] S. Tian, O. Neumann, M.J. McClain, X. Yang, L. Zhou, C. Zhang, P. Nordlander, N.J. Halas, Aluminum nanocrystals a sustainable substrate for quantitative SERS-based DNA detection, Nano Lett. 17 (2017) 5071–5077.
[31] B.-B. Xu, L. Wang, Z.-C. Ma, R. Zhang, Q.-D. Chen, C. Lv, B. Han, X.-Z. Xiao, X.-L. Zhang, Y.-L. Zhang, K. Ueno, H. Misawa, H.-B. Sun, Surface-plasmon-mediated programmable optical nanofabrication of an oriented silver nanoplate, ACS Nano 8 (2014) 6682–6692.
[32] G. Eom, H. Kim, A. Hwang, H.-Y. Son, Y. Choi, J. Moon, D. Kim, M. Lee, E.-K. Lim, J. Jeong, Y.-M. Huh, M.-K. Seo, T. Kang, B. Kim, Nanogap-rich Au nanowire SERS sensor for ultrasensitive telomerase activity detection: application to gastric and Breast cancer tissues diagnosis, Adv. Funct. Mater. 27 (2017) 1701832.
[33] L. Peng, L. Zhang, J. Yuan, C. Chen, Q. Bao, C.W. Qiu, Z. Peng, K. Zhang, Gold nanoparticle mediated graphene plasmon for broadband enhanced infrared spectroscopy, Nanotechnology 28 (2017) 264001–264006.
[34] J.S. Park, N.I. Goo, D.E. Kim, Mechanism of DNA adsorption and desorption on graphene oxide, Langmuir 30 (2014) 12587–12595.
[35] L. Ouyang, Y. Hu, L. Zhu, G.J. Cheng, J. Irudayaraj, A reusable laser wrapped graphene-Ag array based SERS sensor for trace detection of genomic DNA methylation, Biosens. Bioelectron. 92 (2017) 755–762.
[36] M.F. El-Kady, V. Strong, S. Dubin, R.B. Kaner, Laser scribing of high-performance and flexible graphene-based electrochemical capacitors, Science 335 (2012) 1326–1330.
[37] H. Tian, C. Li, M.A. Mohammad, Y.-L. Cui, W.-T. Mi, Y. Yang, D. Xie, T.-L. Ren, Graphene earphones entertainment for both humans and animals, ACS Nano 8 (2014) 5883–5890.
[38] Y. Zhang, X. Yuan, Y. Wang, Y. Chen, One-pot photochemical synthesis of graphene composites uniformly deposited with silver nanoparticles and their high catalytic activity towards the reduction of 2-nitroaniline, J. Mater. Chem. 22 (2012) 7245–7251.
[39] W. Ren, Y. Fang, E. Wang, A binary functional substrate for enrichment and ultrasensitive SERS spectroscopic detection of folic acid using graphene oxide/Ag nanoparticle hybrids, ACS Nano 5 (2011) 6425–6433.
[40] S. He, K.K. Liu, S. Su, J. Yan, X. Mao, D. Wang, Y. He, L.J. Li, S. Song, C. Fan, Graphene-based high-efficiency surface-enhanced Raman scattering-active platform for sensitive and multiplex DNA detection, Anal. Chem. 84 (2012) 4622–4627.
[41] Y. Lu, G.L. Liu, J. Kim, Y.X. Mejia, L.P. Lee, Nanophotonic crescent moon structures with sharp edge for ultrasensitive biomolecular detection by local electromagnetic field enhancement effect, Nano Lett. 5 (2005) 119–124.
[42] H. Jung, M. Park, M. Kang, K.-H. Jeong, Silver nanoislands on cellulose fibers for chromatographic separation and ultrasensitive detection of small molecules, Light Sci. Appl. 5 (2016) e16009–e16009.
[43] Z. Wang, Z. Dong, Y. Gu, Y.H. Chang, L. Zhang, L.J. Li, W. Zhao, G. Eda, W. Zhang, G. Grinblat, S.A. Maier, J.K. Yang, C.W. Qiu, A.T. Wee, Giant photoluminescence enhancement in tungsten-diselenide-gold plasmonic hybrid structures, Nat. Commun. 7 (2016) 11283–22390.
[44] H. Sun, H. Liu, Y. Wu, A green, reusable SERS film with high sensitivity for in-situ detection of thiram in apple juice, Appl. Surf. Sci. 416 (2017) 704–709.
[45] W. Wei, K. Qu, J. Ren, X. Qu, Chiral detection using reusable fluorescent amylose-functionalized graphene, Chem. Sci. 2 (2011) 2050.
[46] W. Xiong, Y.S. Zhou, W.J. Hou, L.J. Jiang, Y. Gao, L.S. Fan, L. Jiang, J.F. Silvain, Y.F. Lu, Direct writing of graphene patterns on insulating substrates under ambient conditions, Sci. Rep. 4 (2014) 4892–4897.
[47] Y.-L. Zhang, L. Guo, H. Xia, Q.-D. Chen, J. Feng, H.-B. Sun, Photoreduction of graphene oxides: methods, properties, and applications, Adv. Opt. Mater. 2 (2014) 10–28.
[48] D.-D. Han, Y.-L. Zhang, Y. Liu, Y.-Q. Liu, H.-B. Jiang, B. Han, X.-Y. Fu, H. Ding, H.-L. Xu, H.-B. Sun, Bioinspired graphene actuators prepared by unilateral UV irradiation of graphene oxide papers, Adv. Funct. Mater. 25 (2015) 4548–4557.
[49] L.J. Wang, M.F. El-Kady, S. Dubin, J.Y. Hwang, Y. Shao, K. Marsh, B. McVerry, M.D. Kowal, M.F. Mousavi, R.B. Kaner, Flash converted graphene for ultra-high power supercapacitors, Adv. Energy Mater. 5 (2015) 1500786.
[50] D.D. Han, Y.L. Zhang, J.N. Ma, Y.Q. Liu, B. Han, H.B. Sun, Light-mediated manufacture and manipulation of actuators, Adv. Mater. 28 (2016) 8328–8343.
[51] X. Yu, H. Cai, W. Zhang, X. Li, N. Pan, Y. Luo, X. Wang, J.G. Hou, Tuning chemical enhancement of SERS by controlling the chemical reduction of graphene oxide nanosheets, ACS Nano 5 (2011) 952–958.
[52] L. Kong, A. Enders, T.S. Rahman, P.A. Dowben, Molecular adsorption on graphene, J. Phys. Condens. Matter. 26 (2014) 443001.
[53] H. Yang, H. Hu, Z. Ni, C.K. Poh, C. Cong, J. Lin, T. Yu, Comparison of surface-enhanced Raman scattering on graphene oxide, reduced graphene oxide and graphene surfaces, Carbon 62 (2013) 422–429.
[54] D.-B. Li, X.-J. Sun, Y.-P. Jia, M.I. Stockman, H.P. Paudel, H. Song, H. Jiang, Z.-M. Li, Direct observation of localized surface plasmon field enhancement by Kelvin probe force microscopy, Light Sci. Appl. 6 (2017) e17038.
[55] Y. Nishijima, K. Ueno, Y. Yokota, K. Murakoshi, H. Misawa, Plasmon-assisted photocurrent generation from visible to near-infrared wavelength using a Au-nanorods/TiO2 electrode, J. Phys. Chem. Lett. 1 (2010) 2031–2036.

Bing Han is currently pursuing her Ph.D. at Jilin University, China. Her research interests include laser printed graphene devices, applications of graphene materials in optical detection, and light-driven bio-inspired robots.

Yong-Lai Zhang received his PhD degree in Chemistry from Jilin University, China, in 2009. He is currently a full professor at Jilin University. His research interests include laser micro-nanofabrication of functional micro-nanostructures, smart actuators, and Bio-MEMS.

Lin Zhu is currently a Master student at Jilin University, China. Her research interest has been focused on laser fabrication of graphene devices and applications in actuators.

Xu-Hui Chen is pursuing his bachelor degree at Jilin University, China. His research interests include stimulus-responsive hydrogels and soft actuators.

Zhuo-Chen Ma received his PhD degree in Electronic Science and Engineering from Jilin University, China, in 2016. He is currently a postdoctor at Jilin University. His research interests include femtosecond laser nanofabrication and metallic micro/nanostructures.

Xu-Lin Zhang is pursuing her Ph.D. at Jilin University, China. His research interests include optical eigenmodes in wave functional materials including photonic crystals, metamaterials, and plasmonics, and their applications in optoelectronic devices, such as in light-emitting devices for efficient light extractions and in solar cells for light trappings.

Jian-Nan Wang is currently pursuing her PhD degree at Jilin University, China. Her research interests lie in the field of biomimetic surfaces.

Wei Wang is currently a Master student at Jilin University, China. Her research interests include functional actuators based on graphene.

Yu-Qing Liu is pursuing her Ph.D. at Jilin University, China. Her research interests lie in the field of biomimetic fabrication, bio-inspired materials, and bionic devices.

Qi-Dai Chen received his PhD degree in Institute of Physics, The Chinese Academy of Sciences, in 2004. He is currently a full professor at Jilin University. His research interests include laser microfabrication, ultrafast laser spectroscopy, photochemistry and photophysics.

Hong-Bo Sun received his Ph.D. in Electronic Science and Engineering from Jilin University in 1996. He worked as a Postdoctoral Researcher at the University of Tokushima, Japan, from 1996 to 2000, and then as an Assistant Professor in the Department of Applied Physics, Osaka University. He became a project leader in 2001. He received an award from the Optical Science and Technology Society in 2002, and won an Outstanding Young Scientist Award issued by the ministry of MEXT (Japan) in 2006. In 2005, he became a Professor (Changjiang Scholar) at Jilin University. His research focuses on laser micro-nanofabrication and their applications in micro-optics, micromachines, microfluids, and microsensors.